Final Report

An Experimental and Numerical Investigation of Turbulent Vortex Breakdown and Aircraft Wakes

Contract NAG 1-1775

Submitted to:

Dr. Thomas B. Gatski
Aerodynamic and Acoustic Methods Branch
Mail Stop 128
NASA Langley Research Center
Hampton, VA 23681

by

Dr. Robert E. Spall
Department of Mechanical Engineering
University of South Alabama
Mobile, AL 36688

August 14, 1996

Table of Contents

1. A Numerical Study of Turbulent Vortex Breakdown within a Circular Tube

Abstract

Solutions to the steady, axisymmetric Reynolds-averaged Navier-Stokes equations have been obtained for turbulent vortex breakdown within a slightly diverging tube modeled after the experimental configuration of Sarpkaya (1995a). Solutions employing both standard and RNG based two-equation turbulence models were obtained, as were solutions obtained using a full differential Reynolds stress model. Inlet boundary conditions were derived from experimental data for the mean flow and turbulence kinetic energy as provided to the author by Sarpkaya (Private Communication). The differential Reynolds stress model predicted well the experimentally determined location of breakdown, whereas both two-equation models failed to even predict the occurrence of breakdown. Failure of the two-equation models is attributed to their inability to accurately account for Reynolds stress anisotropies.

Introduction

The majority of numerical works concerning vortex breakdown have concentrated on low Reynolds number, laminar, axisymmetric (c.f., Grabowski and Berger (1976)) or three-dimensional flows (c.f., Spall and Gatski (1991), Breuer and Hanel (1993)). One of the primary contributions of the numerical works has been to provide insight into the internal structure of vortex breakdown. However, in most technological applications of interest, the vortex breakdown arises within a turbulent swirling flow, and the applicability of these laminar results to those flows is questionable. In fact, Sarpkaya (1995a, 1995b) presented experimental results for vortex breakdown in non-cavitating, high Reynolds number (up to 225,000) swirling flows and considered the resulting breakdown fundamentally distinct from the various (up to six, depending upon the classification) forms of laminar breakdown. These high Reynolds number breakdowns are characterized by the lack of a distinct bubble (immediately following what appears to be the stagnation point the flow expands in a sharp, nominally axisymmetric cone of turbulent flow) and appear to be the most robust of all the breakdown forms. Outside of the combustion community (where the breakdown is referred to as a central toroidal recirculation zone, and where geometries typically include such complicating factors as dilution jets and rapid expansions, c.f. Hogg and Leschziner (1989)) the only existing numerical work aimed at studying the internal structure of turbulent vortex breakdown are those of Bilanin et al. (1977) and Spall and Gatski (1995). The work of Bilanin et al. followed much

along the lines of the steady, laminar axisymmetric calculations of Grabowski and Berger (1976). Spall and Gatski presented results for the unsteady, 3-D turbulent breakdown of an unconfined longitudinal vortex employing the algebraic Reynolds stress model of Gatski and Speziale (1993). Their results showed some qualitative agreement with Sarpkaya's experimental results (i.e., robustness, and a lack of asymmetries) but in the absence of common boundary conditions a closer comparison between the results was deemed unwarranted.

Several distinct approaches to modeling these high Reynolds number swirling flows exist, ranging from solutions to the Reynolds-averaged Navier-Stokes equations, to large eddy simulations (LES), to direct numerical simulations (DNS). However, to date, DNS and LES simulations utilizing spectral schemes have been limited primarily to geometrically simple configurations, and for the case of DNS, the restrictions include relatively low Reynolds numbers (costs scale as the Reynolds number cubed). Higher-order finite-difference techniques enjoy more flexibility in terms of geometries and boundary conditions, but with the lack of spectral accuracy, their built-in low-pass filter may tend to confuse the issue of resolved scales vs. subgrid-scale motions. One must conclude that in the foreseeable future, it is unlikely that LES or DNS approaches will be available as computational tools to be utilized in the investigation and solution of turbulent flow problems in most *technologically important* applications such as wake-vortex alleviation, submarine non-acoustic stealth, and flame stabilization.

Hence, we are motivated in the present study to employ the Reynolds-averaged Navier-Stokes equations (RANS) to study numerically vortex breakdown in high Reynolds number turbulent swirling flows. The geometry is modeled after the axisymmetric diverging tube test section employed in the experimental work of Sarpkaya (1995a, 1995b). Several features contribute to the complex nature of this flow, including the existence of an adverse pressure gradient (diverging tube), body forces arising from the strongly swirling flow, and an internal separation point (at breakdown). Thus, although the geometry is somewhat simplified from that of (for instance) most combustors, many of the features contributing to the complex turbulent flow are present, and it represents an excellent test case to ascertain the capabilities of the RANS. To the extent possible, the suitability of both 2-equation and differential Reynolds stress closure models in predicting these flows will be evaluated.

Numerical Method and Boundary Conditions

The pressure-based finite-volume code Fluent (Fluent, Inc., Lebanon, NH) has been utilized to solve the Reynolds-averaged Navier-Stokes equations. A formulation employing cylindrical-polar velocity components was used to reduce numerical diffusion. Interpolation to cell faces was performed using a blended second-order upwind/central difference scheme (Maruszewski 1991). Pressure-velocity coupling was based upon the SIMPLEC procedure (c.f., Patankar 1980).

Both standard and Renormalization Group (RNG) based $K-\varepsilon$, and differential Reynolds stress models (DSM) have been employed. It is well known that in regions of high strain rate the standard $K-\varepsilon$ model produces excessive levels of turbulence kinetic energy, leading to high values of the isotropic turbulent viscosity. As a result, the model may overpredict the radial diffusion of momentum in strongly swirling flows, leading to an overly rapid decay of maximum swirl velocities. The RNG based models have been shown to produce results superior to the standard $K-\varepsilon$ model for flows with high streamline curvature and strain rate (Yakhot et al. 1992). The RNG model is similar in form to the standard $K-\varepsilon$ model except for the addition of a rapid strain term ($\bar{R}$) in the dissipation equation which is written in cartesian tensor form as:

$$\frac{D\varepsilon}{Dt} = \frac{\partial}{\partial x_j}\left(\frac{\nu_t}{\sigma_\varepsilon}\frac{\partial \varepsilon}{\partial x_j}\right) + 2\nu_t C_{\varepsilon 1}\frac{\varepsilon}{K}S_{ij}^2 - C_{\varepsilon 2}\frac{\varepsilon^2}{K} - \bar{R} \qquad (1)$$

where,

$$\bar{R} = \frac{C_\mu \eta^3(1-\eta/\eta_0)}{1+\beta\eta^3}\frac{\varepsilon^2}{K}. \qquad (2)$$

In addition, $\nu_t = C_\mu K^2/\varepsilon$, $\eta = SK/\varepsilon$, and $S = (2S_{ij}S_{ij})^{1/2}$ (where S_{ij} is the strain rate). (Note that in regions of large strain rate the sign of $\bar{R}$ changes, with the effect of decreasing ν_t.) For the standard $K-\varepsilon$ model, $\bar{R} \equiv 0$. An additional feature of the RNG model is that no empirical constants appear in the equations. Theoretical analysis yields $C_\mu = 0.084$, $C_{\varepsilon_1} = 1.42$, $C_{\varepsilon 2} = 1.68$, $\sigma_\varepsilon = 0.72$, $\beta = 0.012$ and $\eta_0 = 4.38$ (c.f. Yakhot et al. 1992) which may be compared with the values employed for the standard $K-\varepsilon$ formulation of $C_\mu = 0.09$, $C_{\varepsilon_1} = 1.44$, $C_{\varepsilon 2} = 1.92$, and $\sigma_\varepsilon = 1.3$.

We note that in the past, other modifications to the standard $K-\varepsilon$ model have been applied to the dissipation rate equation in an effort to improve predictions for swirling flows. These are primarily (ad-hoc) Richardson number modifications to the sink or source terms, and have met with only limited success (c.f., Srinivasan and Mongia 1980).

The advantage of Reynolds stress models is that they inherently account for the effects of streamline curvature, body forces and rotation. In the present work, the Reynolds stress model closure assumptions are based upon the assumptions provided in Launder et al. (1975) and Gibson and Launder (1978). In particular, the pressure-strain term (Φ_{ij}) is modeled as

$$\Phi_{ij} = -C_1\frac{\varepsilon}{K}\left(\overline{u_i' u_k'} - \frac{2}{3}\delta_{ij}K\right) - C_2\left(P_{ij} - \frac{2}{3}\delta_{ij}P\right) \qquad (3)$$

where $P = \frac{1}{2}P_{ii}$ (and P_{ij} is the production term) and the values of the constants C_1 and C_2 are given as 1.8 and 0.60, respectively. The wall reflection terms responsible for redistribution of the normal stresses near the wall were not included, however this should not be problematic since we are primarily interested in the vortex core region where contributions from these terms would be small. The dissipation term was modeled by an isotropic dissipation rate while diffusion was modeled by a gradient approximation.

For each of the models, standard equilibrium wall functions were used to implement the duct wall boundary conditions. This eliminated the need for an overly fine grid near the wall, which again, is far removed from the primary area of interest—the vortex core region.

The course of the numerical study has been guided by experimental data provided to this investigator by Professor Sarpkaya (Private Communication). In particular, experimental data in terms of the mean flow and turbulence kinetic energy profiles were utilized to derive the inlet boundary conditions. (Lacking further experimental data, for the DSM the Reynolds shear stresses were set to zero. Of course, the turbulence is not isotropic, and in the future it is intended that calculations be performed employing the complete experimental Reynolds stress distribution.) For each of the models the dissipation rate at the inlet was specified through the relation:

$$\varepsilon = C_\mu^{3/4}\frac{K^{3/2}}{l} \qquad (4)$$

where the length scale l was taken as the radius of the vortex core. The inlet distributions of the

mean velocities (where $\bar{u}$ and $\bar{w}$ represent axial and azimuthal velocities, respectively) and the turbulence kinetic energy and dissipation rate are shown in Figs. (1a,b). (Velocities and lengths have been made dimensionless with respect to the inlet mean axial velocity and tube radius, respectively.) Figure (1a) reveals that the core radius (defined as the radius of maximum swirl velocity) at the inlet is approximately 0.06. In addition, the high levels of turbulence kinetic energy associated with the vortex are confined within a radius of approximately 0.12.

Results

The calculations to be presented were performed on a 150x71 grid with significant stretching toward the duct centerline, duct outer wall, and (axially) near the breakdown region. At the inlet, approximately 10 grid points were contained within the vortex core. A grid resolution study, performed by doubling the number of grid points in each direction, did not significantly alter the results. (A comparison between coarse and fine grid calculations is provided later in this section.) All calculations were performed at a Reynolds number (based upon mean axial velocity and tube diameter at the inlet) of 130,000.

Shown in Figs. (2a-c) are contours of mean axial velocities computed using the standard $K-\varepsilon$, RNG based $K-\varepsilon$, and DSM, respectively (with the vertical scales being expanded by a factor of 10 for clarity). We note that the experimentally determined location of breakdown ranges between $x = 3.3$ and $x = 4.6$ (fluctuating somewhat in time). Both the standard and RNG-based $K-\varepsilon$ models failed to predict the occurrence of vortex breakdown. In fact, the models produced quite similar results, with minimum mean axial velocities along the vortex centerline on the order of $\bar{u} = 0.8$. As discussed in the previous section, one explanation for this failure may be due to the dissipative nature of the two-equation models. That is, due to high levels of apparent viscosity the swirl velocities decay so rapidly that the flow remains supercritical (i.e., flow perturbations are swept downstream) and no breakdown occurs. This line of reasoning will be further investigated in the paragraphs to follow.

The full DSM performs much better. Although the flow does not actually stagnate, the characteristic sudden deceleration of the axial velocity is present, and leads to a minimum of $\bar{u} = 0.09$ along the axis at the point $x = 3.33$ (this level of detail is not discernible from the figure). However, whether or not an actual stagnation point occurs in the experiments is still an open

question (Sarpkaya, Private Communication). What is clear however, is the absence of a large bubble-like region that is the hallmark of the observed laminar, nominally axisymmetric breakdowns. Downstream of breakdown, the DSM predicts a very slow recovery of the axial velocity. This behavior is considerably different than that of 2-equation models, which (when sufficient swirl is present to promote breakdown) tend to predict a rapid recovery of the mean axial velocity. Although detailed experimental data is not available, results describing the bounding breakdown "envelope" are reasonably consistent with flow visualization studies of Sarpkaya (1995a, 1995b).

It is also noted that a set of calculation was also performed using the DSM model in which only (inviscid) tangency conditions were enforced at the tube walls. The results were considerably modified, with the location of breakdown moving downstream into the constant radius section of the tube to $x \approx 11.5$. However, the structure of the breakdown (in terms of mean velocity profiles) remained virtually unchanged. Hence, although the tube walls are rather far removed from the vortex core (recall that the radius of the vortex core is roughly 6% of the tube radius) the modeling of the wall boundary layer appears essential if one wishes to accurately predict the location of breakdown. This is likely due to the effect that the no-slip condition has on the circumferential velocity profiles within the tube, and is likely not due to the effects of an increasing displacement thickness. An increasing displacement thickness would tend to accelerate the mean axial velocity and force the breakdown further downstream, opposite the results observed in these calculations.

Shown in Figs. (3a-c) are contours of constant mean circumferential velocity for the standard $K-\varepsilon$, RNG based $K-\varepsilon$ and DSM, respectively. (To increase clarity, only the region $0 \le x \le 5$ is shown.) These results confirm our earlier suggestion that the swirl velocities decay much more rapidly for the 2-equations models than for the DSM. Simply by examining the contour levels one can ascertain that the profiles for the 2-equation models remain supercritical. Hence it is not surprising that no breakdown occurs, and that the centerline axial velocities remain nearly constant over the downstream section of the duct (as shown in Figs. (2a,b)). Also shown in Fig. (3d) are the results for the DSM calculated using a 300x140 grid. Clearly, no significant changes in the results occurred, and the original grid resolution was deemed adequate. (High resolution calculations for each of the 2-equation models also confirm the adequacy of the original resolution.)

The interesting question concerns whether or not high levels of diffusivity are responsible

for the poor performance of the 2-equation models. We attempt to answer this question by examining contours of constant turbulence kinetic energy, in Figs. (4a-c), and apparent viscosity, $C_\mu K^2/\varepsilon$, in Figs. (5a-c). In terms of the turbulence kinetic energy, the results for each of the 3 models are similar. In fact, the $K-\varepsilon$ model predicts levels of turbulence kinetic energy closer to the DSM than does the RNG model. Recall that the RNG model includes a rapid strain term, and different values for the coefficients (specifically, $C_{\varepsilon 2}$) such that it tends to predict lower levels of turbulence kinetic energy than does the standard model. We see that trend here, albeit the lower levels predicted by the RNG model are not predicted by the DSM. (Although it is not suggested that the DSM should set the standard for comparison.)

Combined with the dissipation rate, these profiles of turbulence kinetic energy can be used to compute the apparent turbulence viscosity, shown in Figs. (5a-c). Here, the levels of turbulence kinetic energy predicted by the RNG model are manifested in notably decreased levels of apparent viscosity. For instance, over the region in which we expect the breakdown to form $(2 \le x \le 3)$ the RNG model predicts levels of ν_t approximately 2.5 times below that of both the standard $K-\varepsilon$ and DSM models. In fact, the distribution of ν_t for the $K-\varepsilon$ and DSM models is quite similar. Yet, this difference in the apparent viscosity between the 2-equations models is not manifested as a notable difference between the respective mean velocity profiles. Hence, it does not seem that the failure of the 2-equation models should be attributed solely to excessive levels of apparent viscosity. Rather, it is more likely that the failure of these models should be attributed to their inability to properly account for Reynolds stress anisotropies.

Conclusions

In summary, the Reynolds stress model appears to predict quite well the location of the onset of turbulent vortex breakdown in a slightly diverging pipe, based upon the experimental results, provided to this author by Professor Sarpkaya. This result is quite encouraging in that only profiles for the mean flow and turbulence kinetic energy were available as inlet boundary conditions. (Even these quantities are not likely to be available in most industrial applications involving turbulent swirling flows.) In addition, the lack of a large recirculation region agrees qualitatively with experimental results. It also turned out that the inclusion of no-slip wall boundary conditions had a large effect on the predicted location of breakdown.

As expected, the performance of the 2-equation $K-\varepsilon$ models was totally inadequate, and their use for vortex breakdown flows must be discouraged. However, rather than attributing the failure of the 2-equation models on excessive diffusivity, it is concluded that the real problem likely lies in the failure of the 2-equation models to accurately predict the Reynolds stress anisotropies. Pending the availability of experimental data, future work will concentrate on more quantitative aspects of the DSM predictions, such as a comparison between experimental and numerical results for the Reynolds stresses upstream and downstream of breakdown.

2. Literature Review: Navier-Stokes Solutions for the Tip-Vortex Problem

Tip vortices shed from finite span lifting surfaces are of considerable technological importance. For example, tip vortices contribute to the induced drag of the generating surface, a situation that is exasperated for low aspect ratio surfaces such as marine propellers. The pressure driven flow about the tip of the lifting surface also decreases the efficiency of fluid dynamic devices such as axial compressors and turbomachine blades. Perhaps the application that has received most attention is the "wake-vortex interaction" problem in which trailing wing-tip vortices pose a hazard to smaller following aircraft. In fact, the FAA dictates the frequency of aircraft take-offs and landings at the nation's airports by accounting for the presence and demise of these lift-generated vortices. Another vortex-structure interaction problem of considerable importance is the blade-vortex interaction that occurs when vortices shed from a helicopter rotor blade interact with a following blade. The resulting large, unsteady forces may attribute to premature blade failure.

Vortex-structure interaction problems have received considerable attention from the aerospace industry. Of primary interest here is the wake-vortex problem, and in particular, efforts at computational simulations of the tip-vortex. Computational efforts in this area have been ongoing for only about a decade, which is a testimony to the difficulties inherent in the problem. These difficulties are two-fold. First, the computational resources required to attack the problem are considerable, limiting the earliest calculations which were performed on Cray 1 and Cray XMP class machines. Second, and equally important, the structure of the turbulence within the tip-vortex is highly non-isotropic, and thus turbulence models typically used in wall bounded aerodynamic flows such as the Baldwin-Lomax model are not adequate to model the tip vortex. These are the primary issues of concern. Progress made in addressing these (and closely related) issues over the past decade will be discussed in the paragraphs to follow.

One of the earliest sets of calculations were those of Mansour (1985) in which the thin-layer Navier-Stokes equations were solved for the flow over a low aspect ratio swept wing at a free stream Mach number of 0.8, with the turbulence viscosity being computed using a two-layer Baldwin-Lomax model. Srinivasan et al. (1988) solved the thin-layer Navier-Stokes equations with a Baldwin-Lomax turbulence model for the flow over several different wings, with several different tip configurations. The above studies showed reasonable agreement with surface pressures, however no comparisons between numerical and experimental results were presented for

the structure of the resultant tip vortex. However, with the fairly coarse grids employed (in the region of the vortex core) and by modeling the turbulence viscosity using a Baldwin-Lomax turbulence model, considerable differences would undoubtedly exist.

An effort to address some of the modeling and resolution difficulties inherent in the above studies was made in Dacles-Mariani et al. (1995). They obtained solutions to the full Navier-Stokes equations using the INS3D-UP code (Rogers 1991) with a modified version of the 1-equation turbulence model of Baldwin-Barth (1990). (The production term was modified in an effort to suppress the eddy viscosity in the vortex core.) The airfoil section consisted of a NACA 0012 with a rounded tip and an aspect ratio of 0.75. In essence, they were attempting to model the experiments of Chow et al. (1991) which took place in the 32 in. x 48 in. low speed wind tunnel at the Fluid Mechanics Laboratory of NASA Ames Research Center. That experimental study essentially provided the first set of data available for use in validating numerical models of the near field tip vortex. Due to the relatively large wind-tunnel blockage by the model, the tunnel walls were included in the numerical simulation. Several distinct problems were solved in this work: 1) a wake case in which experimental data for the velocity profiles on a crossflow plane at the trailing edge of the wing was imposed as the inlet boundary conditions, 2) an analytical vortex case (Rott vortex) used to investigate grid resolution, and 3) the complete geometry (at a chord Reynolds number of 4.6 million). The results of the wake case indicated that 3rd-order differencing for the convective terms was too dissipative for the grids considered. Results from the analytical vortex case indicated that 15-20 grid points are needed in the vortex core region to adequately resolve the flow. This translated to a grid spacing of approximately $5x10^{-3}c$ (where c is the chord) in the region of the vortex core. Based upon the above results, calculations for the complete geometry were computed using a fifth-order scheme, with grid spacings in the vortex core of $O(5x10^{-3}c)$. Converged results took on the order of 25 hours of Cray C90 time. In general their results, in terms of surface pressures and streaklines, compared will with experimental data. However, the tip vortex formation was still not sufficiently predicted.

Most recently, Hsiao and Pauley (1996) investigated the tip vortex formation over a NACA 0015 rectangular airfoil with a rounded tip of aspect ratio 3. They too employed the INS3D-UP code with fifth-order upwinding of the convection terms. Their numerical results were compared with the experimental data of McAlister and Takahashi (1991) at a Reynolds number of 1.5 mil-

lion and at an angle of attack of $12°$. One significant difference in their grid generation procedure was that a two block H-H grid was employed, with more grid points being allocated to the upper (suction side) block. They report that, within the vortex core, at least 17 grid points were included in the crosswise direction and 28 points in the spanwise direction. The primary result to come out of this study is that the Baldwin-Barth turbulence model can not be expected to adequately model the wing tip vortex, and that higher-order turbulence modeling will likely be required. This result will undoubtedly become even more apparent as calculations such as these are extended beyond a few chords downstream from the trailing edge. In that case, one- and two-equation models (such as the standard $K-\varepsilon$ model) can be expected to vastly overpredict the rate of decay of the vortex.

The above few studies essentially represent the state-of-the-art in the numerical prediction of the formation of wing tip vortices. We mention that similar work has been performed for the formation of the tip vortex off helicopter rotor blades. The numerical procedure and requirements are essentially identical to the fixed wing case, with the exception of the possible (complicating) inclusion of the rotor wake. The existing studies include those of Srinivasan and McCroskey (1988), Wake and Sankar (1989) and Srinivasan et al. (1992). However, these studies all suffer from the same deficiencies as the earlier fixed wing studies; that is low resolution and/or inadequate turbulence modeling. The studies of Srinivasan and McCroskey (1988) and Srinivasan et al. (1992) also were limited to solutions of the thin-layer Navier-Stokes equations. To summarize, the following issues and/or conclusions have arisen from studies over the last decade of the near-field wing-tip vortex:

1) Turbulence modeling. To date, the "best" turbulence model that has been applied to the near-field wake-vortex problem is a modified form of the 1 equation Baldwin-Barth model. Higher-order models need to be implemented.

2) Grid resolution. Grid resolution requirements within the vortex core are extremely demanding. A minimum of 10 grid points should be placed within the vortex core, the radius of which is on the order of a few percent of the wing chord. Grid spacings to the first point off the wing of $O(10^{-6})c$ to $O(10^{-5})c$ are required.

3) Higher-order differencing schemes. Second- and third-order upwind schemes for the convection terms may be too diffusive (for grid densities that are attainable with todays computer hardware).

4) Differences in the flow fields due to different wing-tip caps are confined to the outer 5% to 10% of the wing span. However, in this region the differences can be significant.

5) Experimental data. Reliable experimental data, including detailed measurements of the individual Reynolds stress components within the tip vortex, are needed to further verify the numerical models.

3. Preliminary Work on Numerical Calculations of the Near-Field Wing-Tip Vortex

A long term study concerning the formation and dissipation of wing-tip vortices has been initiated. The study is being divided roughly into two related problems: 1) the formation of the near field wing-tip vortex, and 2) the far-field vortex, including mechanisms of demise. The problems inherent in numerical simulations of the near field vortex have been outlined in the literature search. Clearly, proper prediction of the vortex structure in the near field is required before an attempt to predict the decay of the vortex structure over hundreds of chords downstream is undertaken. Problems that will undoubtedly manifest themselves in predicting the far field include turbulence modeling and resolution. As with the near field prediction, proper accounting for Reynolds stress anisotropies is a necessity if one is to avoid the overly diffusive solution inherent in standard $K-\varepsilon$ modeling assumptions (as was demonstrated in Section 1).

Predicting the vortex bursting event presents its own set of problems. The bursting phenomena takes place over length scales on the order of the vortex core. In regions far removed from local "events" such as bursting, the flow is essentially parabolic in the streamwise direction. In the region of bursting, the flow is elliptic. However, a priori prediction of the location of a burst event is not possible, and this presents modeling problems from the standpoint of computational efficiency. This problem has not been addressed in the work to date.

Currently, an effort is being made to model the steady, near field vortex structure (which will provide inlet boundary conditions for modeling the far wake region) using a standard high Reynolds number $K-\varepsilon$ model, and the algebraic Reynolds stress model of Gatski and Speziale (which fits into the 2-equation framework) as implemented in the ISAAC code. The effort will attempt to quantify differences in the vortex structure and decay rate as predicted by the two models. Upon completion of these calculations, a full differential Reynolds stress model will be implemented. Initial results are being computed for a NACA 0015 square tip airfoil at a Reynolds number of 1.5 million. This configuration has been chosen due to the relatively large amount of (near field) experimental data available in the work of McAlister and Takahashi (1991) (this case represents their "baseline"). An initial coarse H-C grid structure has been generated with 105 points in the streamwise direction, 51 points in the wall normal direction, and 93 points in the spanwise direction. A representation of this wing/grid configuration is shown in Fig. 6. Adequate grid reso-

lution in the vortex core region is quite important, and local grid refinement in the core area will be performed to ensure a grid converged solution. Preliminary results for this configuration obtained using a $K-\varepsilon$ model are shown in Fig. 7 in terms of velocity vectors (on the plane $x = 1.1$, where 1.0 represents the trailing edge of the airfoil). Work in the immediate future will concentrate on improved grid clustering in the vortex core region, a task that is not trivial since the vortex quickly migrates inboard as it forms over the wing and trails downstream.

4. References

Baldwin, B.S. and Barth, T.J. (1990) "A One-Equation Turbulence Transport Model for High Reynolds Number Wall-Bounded Flows," NASA TM-102847.

Bilanin, A.J., Teske, M.E. & Hirsh, J.E. (1977). Deintensification as a consequence of vortex breakdown. In *Proceedings of the Aircraft Wake Vortices Conference,* Report No. FAA-RD-77-68.

Breuer, M. and Hanel, D. (1993) "A dual time-stepping method for 3-D viscous incompressible vortex flows," Comput. Fluids, Vol. 22, pp. 467-484.

Chow, J.S., Zilliac, G.G., and Bradshaw, P. (1991) "Initial Roll-Up of a Wingtip Vortex," *Proceedings of the Aircraft Wake Vortices Conference*, Vol. 2, Federal Aviation Administration, Washington, DC, pp. 35-1—35-17.

Dacles-Mariani, J., Zilliac, G.G., Chow, J.S., and Bradshaw, P. (1995) "Numerical/Experimental Study of a Wingtip Vortex in the Near Field," AIAA J., Vol. 33, pp. 1561-1568.

Gatski, T.B. and Speziale, C.G. (1993) "On Explicit Algebraic Reynolds Stress Models for Complex Turbulent Flows," J. Fluid Mech., Vol. 254, pp. 59-78.

Gibson, M.M. and Launder, B.E. (1978) "Ground Effects on Pressure Fluctuations in the Atmospheric Boundary Layer," J. Fluid Mech., Vol. 86, pp. 491-511.

Grabowski, W.J. and Berger, S.A. (1976) "Solutions of the Navier-Stokes Equations for Vortex Breakdown," J. Fluid Mech., Vol. 75, pp. 525-544.

Hogg, S. & Leschziner, M.A. (1989). Computation of highly swirling confined flow with a Reynolds stress turbulence model. AIAA J. 27, 57-63.

Hsiao, C-T. and Pauley, L.L. "Numerical Study of the Tip Vortex Flow over a Finite-Span Hydrofoil," Proceeds of the ASME Fluids Engineering Meeting, San Diego, CA, FED-Vol. 238, pp. 65-74.

Launder, B.E., Reece, G.J., and Rodi, W. (1975) "Progress in the Development of a Reynolds-Stress Turbulence Closure," J. Fluid Mech., Vol. 68, pp. 537-566.

Mansour, N.N. (1985) "Computation of the Tip Vortex Off a Low-Aspect Ratio Wing," AIAA J., Vol. 23, pp. 1143-1149.

Maruszewski, J.P. (1991) "Bounded QUICK Scheme in FLUENT," Fluent, Inc. Technical Memo, TM-049.

McAllister, K.W. and Takahashi, R.K. (1991) "NACA0015 Wing Pressure and Trailing Vortex Measurements," NASA Technical Paper 3151.

Patankar, S.V. (1980) Numerical Heat Transfer and Fluid Flow, Washington, D.C., Hemisphere Publishing Corp.

Rogers, S.E., Kwak, D., and Kiris, C. (1991) "Steady and Unsteady Solutions of the Incompressible Navier-Stokes Equations," AIAA J., Vol. 29, pp. 603-610.

Sarpkaya, T.G. (1995a) "Vortex Breakdown and Turbulence," AIAA 95-0433.

Sarpkaya, T.G. (1995b) "Turbulent Vortex Breakdown," Phys. Fluids, Vol. 7, pp. 2301-2303.

Spall, R.E. and Gatski, T.B. (1991) "Computational Study of the Topology of Vortex Breakdown," Proc. R. Soc. Lond. A Vol. 435, pp. 321-337.

Spall, R.E. and Gatski, T.B. (1995) "Numerical Calculations of Three-Dimensional Turbulent Vortex Breakdown," Int. J. Numer. Methods Fluids, Vol. 20, pp. 307-318.

Srinivasan, R. & Mongia, H.C. (1980). Numerical computation of swirling recirculating flows. NASA CR-165196.

Srinivasan, G.R., Baeder, J.D., Obayashi, S., and McCroskey, W.J. (1992) "Flowfield of a Lifting Rotor in Hover: A Navier-Stokes Simulation," AIAA J., Vol. 30, pp. 2371-2378.

Srinivasan, G.R. and McCroskey, W.J. (1988) "Navier-Stokes Calculations of Hovering Rotor Flowfields," J. Aircraft, Vol. 25, pp. 865-874.

Srinivasan, G.R., McCroskey, W.J., Baeder, J.D., and Edwards, T.A. (1988) "Numerical Simulation of Tip Vortices of Wings in Subsonic and Transonic Flows," AIAA J., Vol. 26, pp. 1153-1162.

Wake, B.E. and Sankar, L.N. (1989) "Solutions of the Navier-Stokes Equations for the FlowAbout a Rotor Blade," Journal of the American Helicopter Society, Vol. 34, pp. 13-23.

Yakhot, V., Orzag, S.A., Thangam, S., Gatski, T.B. and Speziale, T.B. (1992) "Development of Turbulence Models for Shear Flows by a Double Expansion Technique," Phys. Fluids A, Vol. 4, pp. 1510-1520.

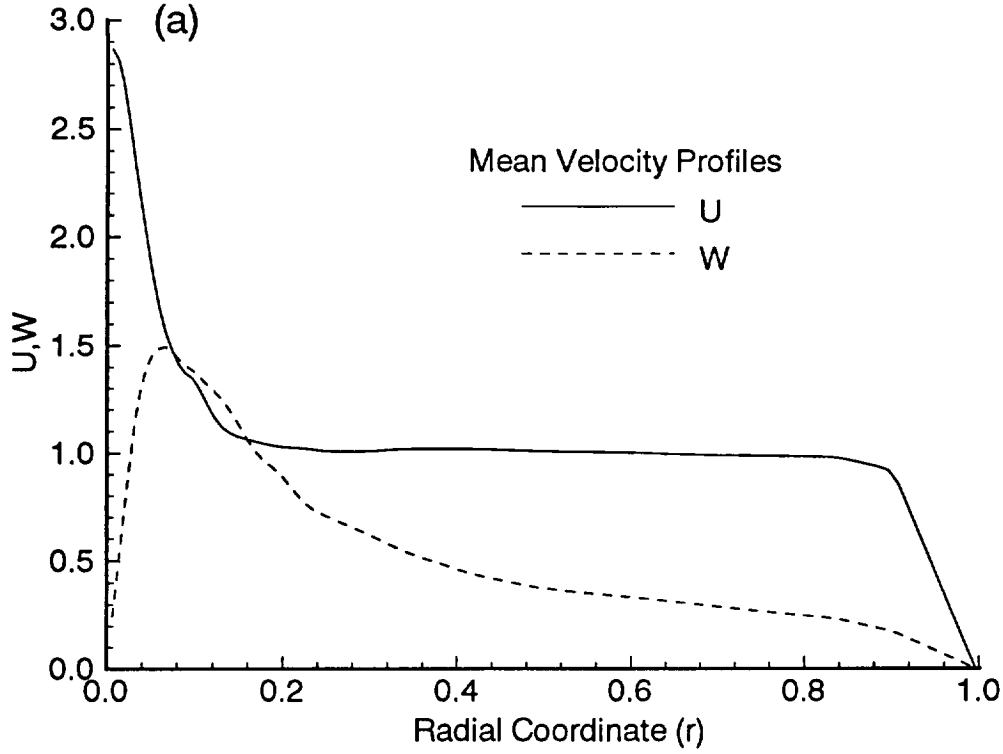

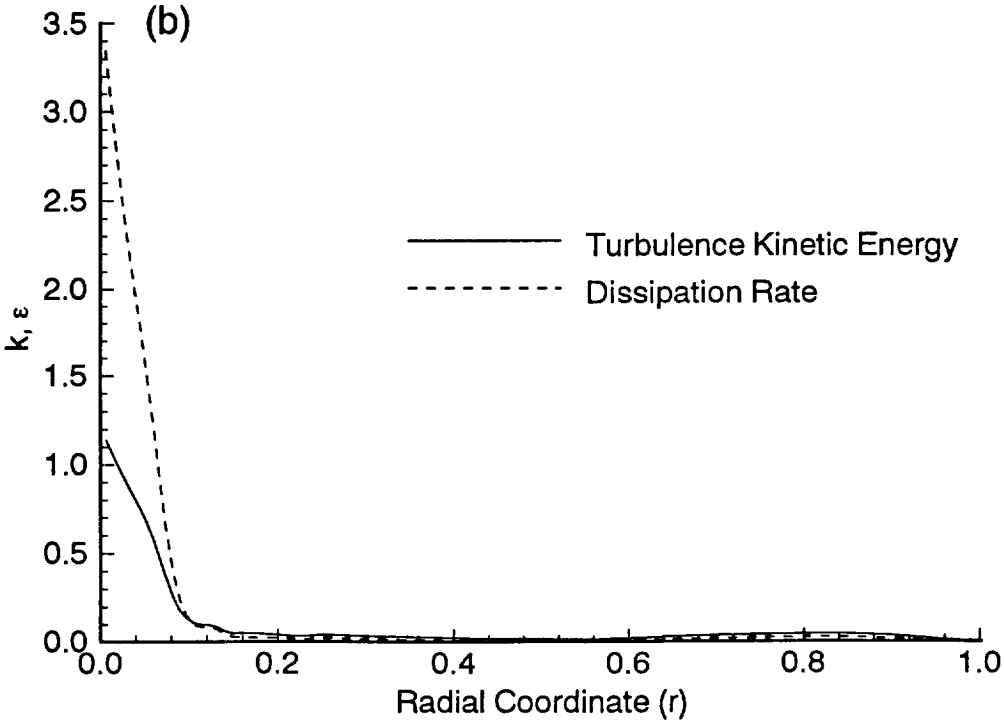

Figure 1. Experimental profiles utilized as inlet boundary conditions.

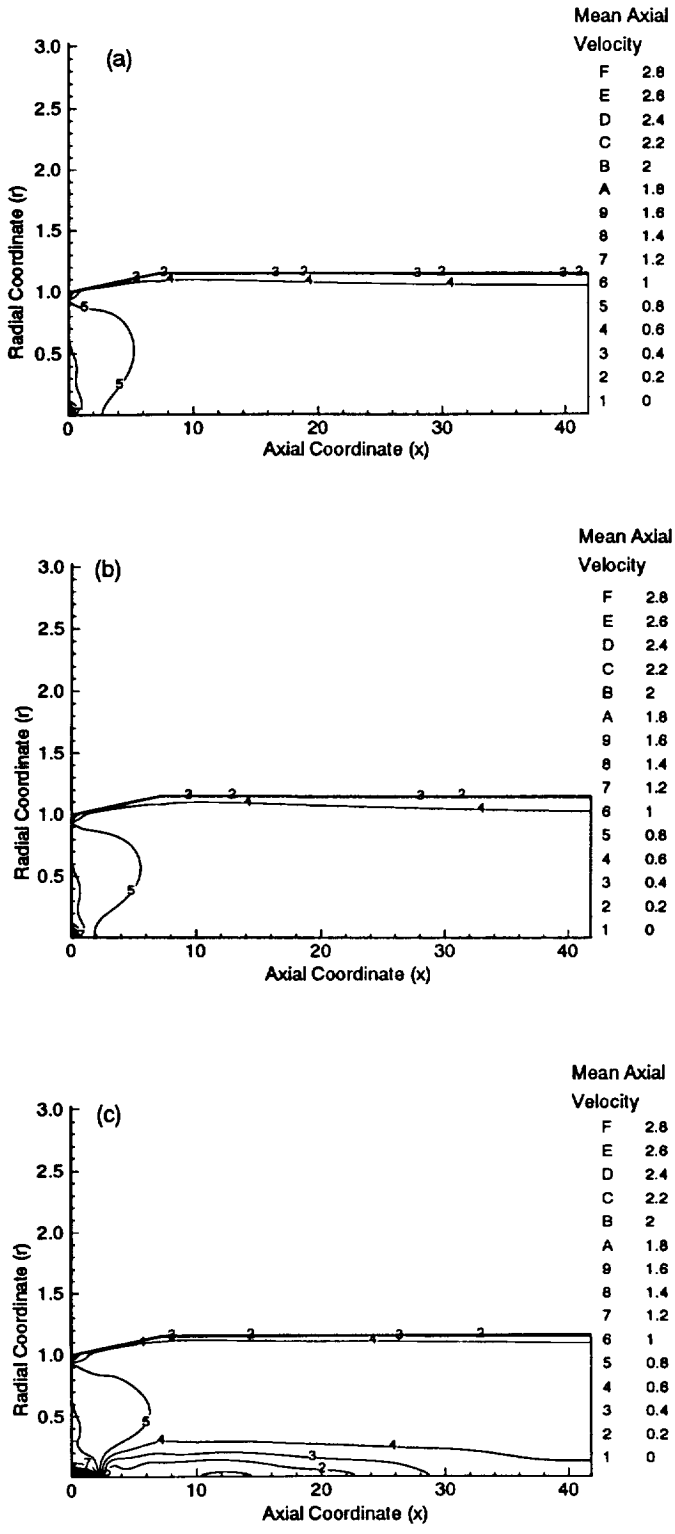

Figure 2. Contours of constant mean axial velocity.

a) $K-\varepsilon$ model

b) RNG-based $K-\varepsilon$ model

c) differential Reynolds stress model

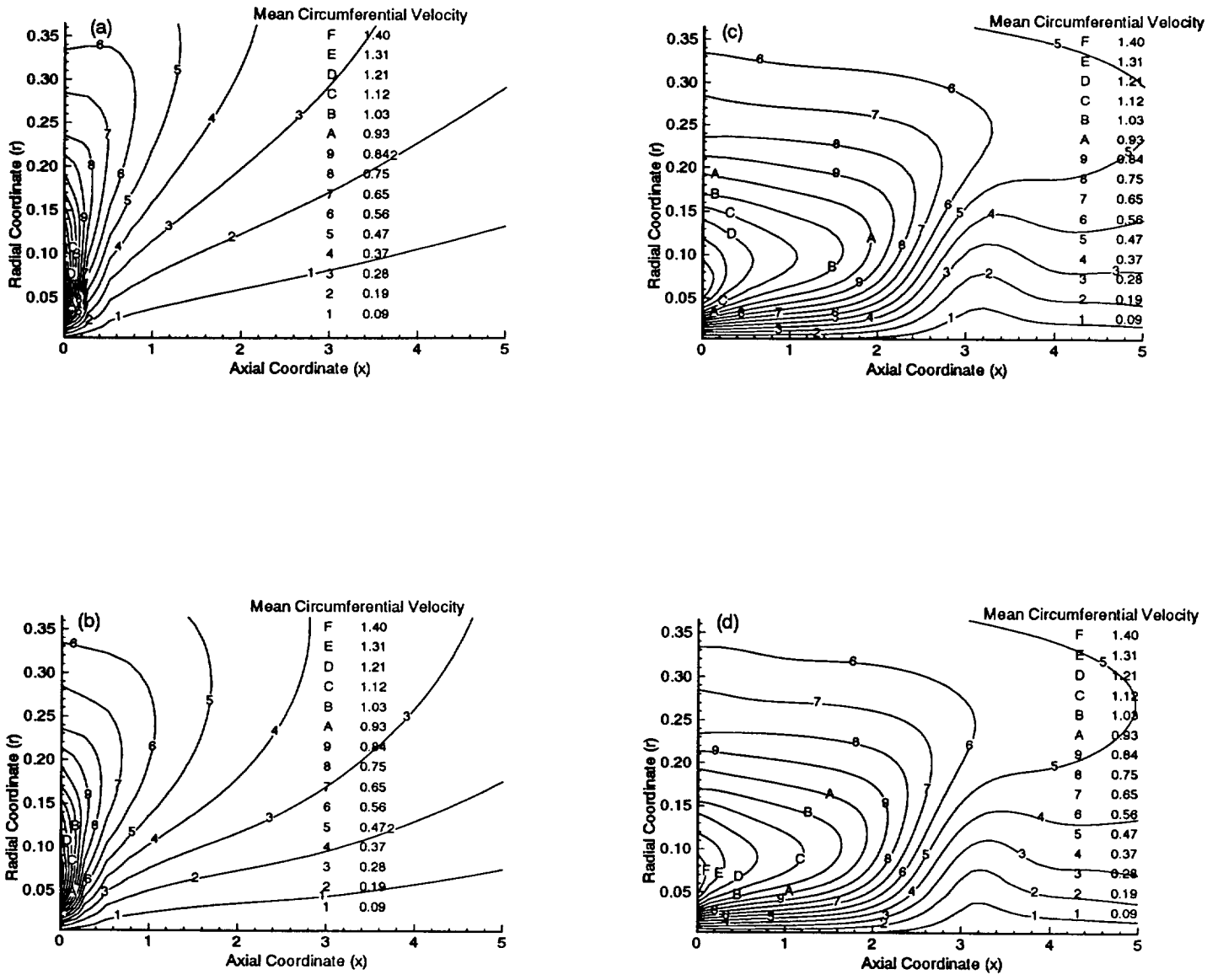

Figure 3. Contours of constant mean circumferential velocity.

a) $K-\varepsilon$ model

b) RNG-based $K-\varepsilon$ model

c) differential Reynolds stress model (150x71 grid)

d) DSM on a 300x140 grid

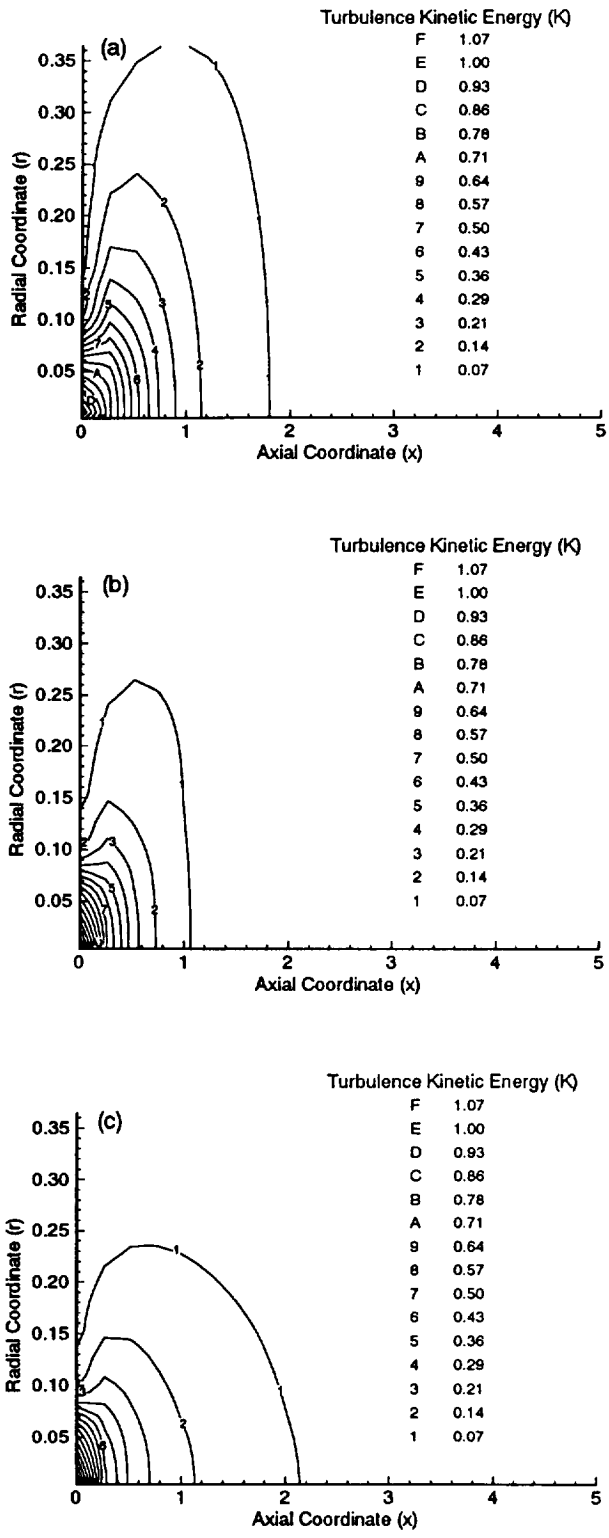

Figure 4. Contours of constant turbulence kinetic energy.

a) $K-\varepsilon$ model

b) RNG-based $K-\varepsilon$ model

c) differential Reynolds stress model

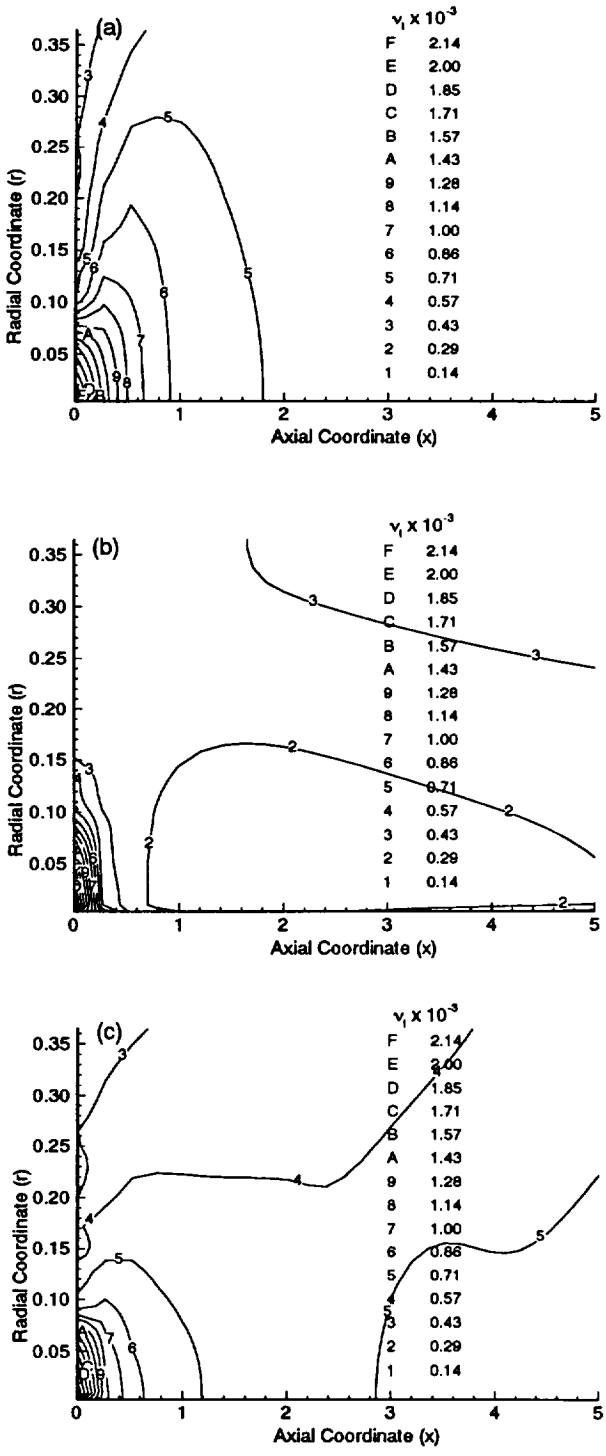

Figure 5. Contours of constant turbulent viscosity.

a) $K-\varepsilon$ model

b) RNG-based $K-\varepsilon$ model

c) differential Reynolds stress model